Two Examples of Using Machine Learning for Processing Sensor Data of Capacitive Proximity Sensors

Björn Hein[1⋆] and Hosam Alagi[2]

[1] Karlsruhe University of Applied Science
bjoern.hein@hs-karlsruhe.de
[2] Karlsruhe Institute of Technology
hosam.alagi@kit.edu

Abstract. Recently we have shown developments on capacitive tactile proximity sensors (CTPS) in combination with machine learning techniques to extract further information out of the sensor signals. In this work we summarize two examples of the applications we have presented. In the first approach we have investigated distance classification based on the proximity information of the sensors. In the second approach the possibility of material recognition was investigated. The latter is done by variating the spatial resolution and the exciter frequency of our sensors. For both approaches, distance classification and material recognition, an artificial neural network was set up and fed with various data sets of different electrode combination. The influence of the electrode combinations and shapes on the recognition accuracy was investigated and some promising results could be achieved.

1 Introduction

An established sensor technology, at least in research, are sensor skins for robots. These can detect touch and provide information about location and force of this touch. These skins are used for a variety of applications ranging from human-robot-interaction (HRI) and grasping concepts. More recently the ability to detect objects/events in the near proximity of the robot are under investigation as they provide the interesting possibility to get information right before the touch event even happens. This extends even further the possibilities in HRI, grasping and could significantly contribute to safety concepts. Proximity sensing closes in a unique way the perception gap between classical vision based sensing and touch sensing.

For the implementation of this proximity sensor modality different measurement principles have been proposed based on different physical effects, mainly acoustic, optical and capacitive; examples are [1–3].

Our line of work has been dedicated to designing hardware and applications for capacitive tactile and proximity sensing. Capacitive sensing is affected by the electrical properties of the object (conductivity, permittivity when non-conducting), its size and shape and of course its distance to the sensor. Unfortunately this implies complicated dependencies in the sensor signals, which are not easy modeled.

The research presented here is a continuation of our previous work [4], where we introduced a flexible, easy to integrate capacitive tactile proximity sensor for applications in robotics (s. Fig. 1).

⋆ This research was funded by the German Research Foundation (DFG) under the grants HE 7000/1-1 and WO 720/43-1.

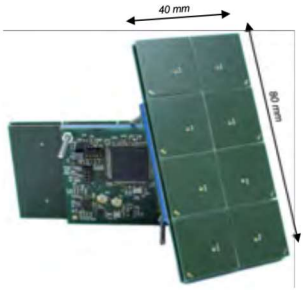

Fig. 1. Sensor module and electrodes of the sensor presented in [4]. Up-to eight electrodes can be combined individually.

In this work we especially summarize two aspects of our previous research, which did focus on using machine learning techniques for extending distance measurement [5] and material recognition [6].

The rest of the paper is structured as follows: After this introduction the state of the art is presented in Section 2. In Section 3 we present our sensing system used to collect the data about the different objects. In Section 4.1 we discuss the experiments in material recognition and their results. Finally, in Section 5, we provide a summary and give conclusions for this paper.

2 Related Work

A very interesting application scenario for proximity sensing is preshaping of a robot end-effector, i.e. aligning the gripper of a robot to an object prior to finally grasping it. Preshaping applications for robotic gripper have been shown based on proximity sensing with capacitive sensors in [7–9]. Another important application for proximity sensing is collision avoidance. Early works are [10] and the milestone work by Lumelsky and Cheun [11]. As mentioned above, capacitive sensing is susceptible to shape, material and size of the objects it perceives and suffers from strong non-linearity. Therefore machine learning seems to be a valid way to address these issues.

Like it was stated in the introduction, the second aspect to be presented in this work is material classification. Capacitive proximity measurements have the potential to be applicable also for this kind of scenario. Materials can basically categorized and distinguished by their relative permittivity ε_r. In general this can be done by gathering sample data and then applying classical classification methods. Kirchner et al. proposed data generated by using three discrete frequencies [12] to classify four classes of objects (concrete, human, metal and wood). The use of different frequencies is decisive for their results. By driving the sensor towards the object, a distance dependent curve was recorded which was then used for the material ranging. In our work we also use different frequencies, but we propose an approach which only depends on the sensor values. In other words, a single frame of sensor measurements is used to predict the material.

Another interesting approach for an impedance analyzer using magnetic and electric component is shown by Yunus et al. and Wang et al. [13] and [14] respectively. Both works target the same application domain regarding water pollution detection. Wang et al. specifically investigated different electrode designs in [14]. Due to the fact that significant changes in the signal have been observed in permittivity at frequencies below 500 kHz and that the shape and the order of the electrodes are major for the measurement, we see the analogy to our sensor in the multi-frequency measurement and the dynamic electrode

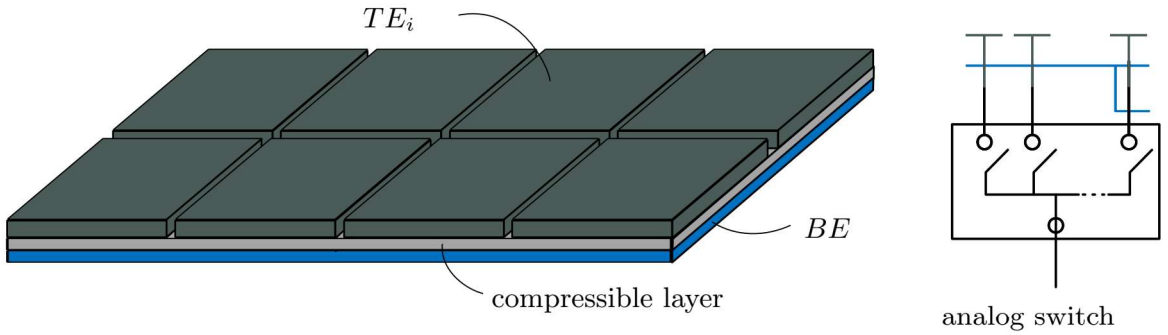

Fig. 2. The assembly of a sensing element (TE_i - Top Electrode i, BE bottom electrode. An analog switch allows selection and combination of electrodes [4].

configuration. However, our approach is less complex using two discrete frequencies and the electrode reshaping was realized by the flexible spatial resolution of the sensor.

A simple capacitive proximity sensor with one exciter frequency and fixed electrodes would not provide enough information about detected objects. Therefore, A.Kimoto in [15] combined optical sensor with capacitive one. He was able to distinguish between Acrylic, PTFE, Class and Aluminum in different surface properties. In the context of robotics and especially in grasping applications collecting information about the object is essential. In such scenarios a gripper or manipulator equipped with suitable capacitive sensors can provide internal properties of the object's material. Respectively, the control system can then decide which object should be grasped [16]. In this case the capacitive sensor provides information which is complementary to those of vision or haptics.

3 System Description

The sensor design, which was presented in detail in [4] (s. Fig. 1), can be used in a very flexible manner, in this section we therefore start with presenting the general concept of our sensor design and then explain the hardware implementation needed for the two approaches: distances measuring and material classification.

3.1 Sensor Design

One specialty of our sensor is its ability to reconfigure its spatial resolution on-line by merging the electrodes using an analog switch (s. Fig. 2). This increases the measurement area of the resulting electrode and thus the sensitivity of the measurement. Additionally the sensor is able to use different frequencies for the measurement and multiple sensors can by used in a synchronized fashion. Fig. 5 shows in the material classification task three of our sensor modules as part of an end-effector that is approaching a wooden ball.

The sensor can be used in *self-capacitive* (send) and *mutual-capacitive* (receive) mode. Both modes are alternatively called *single-ended* and *double-ended* in literature. In the self-capacitive mode the top electrodes (TE_i) are driven with an AC signal passing through the analog switch, which can select or join electrodes arbitrarily. The signal causes the periodic charging and discharging of the electrodes. The capacitive coupling of the configuration with the environment can be measured by finding the amplitude of the current flowing through the circuit. To guide the coupling towards the "outside" side of the sensor, the bottom electrode BE is used to actively shield the TE_i from any

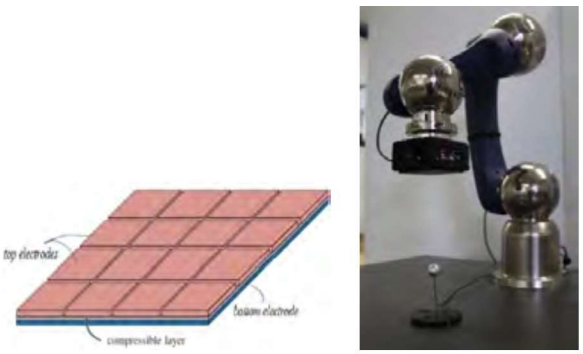

Fig. 3. First sensor setup for investigating distance measurement based on machine learning. Left: $4x4$-sensor configuration using 2 sensor modules controlling $2x4$ electrodes at a time; Right: Schunk-LWA with $4x4$-sensor configuration attached as end-effector.

components below. An object will affect the coupling according to its material properties and its proximity to the sensor. In the mutual-capacitive receive mode the TE_i are connected to ground through a measurement circuit. In the presence of a sender there will be an electric field lines showing from the sender towards the receiver, inducing a current at the receiver side. An object near the electrodes will affect the field. This effect is reflected in the current being measured and again depends on the object properties. This double-ended measurement is suited for detecting insulated objects with a high enough relative permittivity. With our sensor a tactile measurement is also possible due to the compressible, insulating layer between TE_i and BE, but it is not used in this work. Finally, the frequency of the exciting signal can be adjusted, which is also an important aspect, i.e. for material recognition, since the permittivity can be a frequency dependent value.

For both setups the end-effectors with the sensors were mounted on small 6-Axes-Robots. Distance measurement tests were done with a SCHUNK-LWA (s. Fig 3, right), material classification tests where done using an UR5 (s. Fig. 5, top right) and the Robot Operating System *(ROS)* was used as a middleware. For generating and executing the trajectories *MoveIt* and *ROS Control* were used.

3.2 Sensor configuration

Sensor setup for evaluating distance measurements via machine learning
For the machine learning approach measuring distances 2 sensor modules with 2x8 electrodes were used as sensing elements (s. Fig. 3). In this setup the end-effector consists of 16 electrodes and the spatial resolution is used to take measurements with different electrode and sizes, i.e. signals from one single electrode or signals from 4 combined electrodes were recorded. So, a total of 22 different signals were collected. The basic idea behind this approach is that with a higher resolution (single electrodes) we get shorter measurement range and a higher uncertainty about the capacitances and therefore distances, but the object's size and localization is clearer. Conversely, with lower resolution (combined electrodes) we get a higher measurement range due to a better representation of the capacitance and therefore distances at the cost of loosing accuracy in the localization of the object. A frame combining both potentially unifies the advantages of both worlds.

The used end-effector for material detection is basically quite similar to the one for distance measurements and can be seen in Fig. 5. Two 4×2 modules combined make

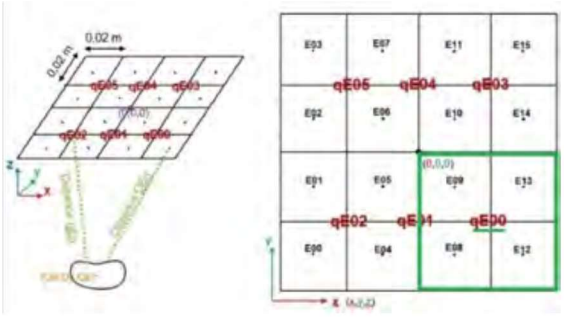

Fig. 4. Sensor configuration used for testing distance measuring [5]. Due to the flexibility in the combination of electrodes (s. Fig. 2) the signal of single electrodes ($E00 - E16$) and combined electrodes ($qE00 - qE05$, 4 combined electrodes) are fed to the neuronal network.

up the receiver array of the end-effector as already shown in the distance measurement set-up (s. Fig. 3). In addition a third module was added and acts this time as dedicated sender. Six of its electrodes are installed at both sides of the receiver array, but only the ones closest to the receivers have been activated (represented by blue stripes). The flexible spatial resolution is used to take measurements with different electrode sizes and shapes, as seen Fig. 5($C1_n$, $C2_m$, $C3_k$). At each resolution the set of measurements can be thought of as a capacitive image. The collection of all measurements then is a multi-resolution capacitive image, which we call a *frame*. The hardware sequentially generates a frame within some fraction of a second by time-multiplexing through each configuration of electrodes.

Sensor setup for evaluating material detection via machine learning

By reshaping the electrodes we assume to get different configuration of the potential field and thus the penetration or polarization of the dielectric objects. in addition two exciter frequencies were used to obtain information about the object material due to the fact that the relative permittivity shows a frequency dependency. Figure 5 shows the configurations used for the measurements, where three basic electrode combinations are highlighted.

4 Evaluation and Results

4.1 Experimental Setup: Distance measurements

Basic idea of this experiment was to classify distances according to 1cm steps. To generate the training data the end-effector (s. Fig. 3) was moved over the object in the pattern shown in Fig. 6.

In this section we discuss the experimental setup, the framework and setup for learning with artificial neural networks (ANNs) and the results obtained using different combinations of electrode configurations and signal frequencies. The latter - changing frequencies - was only used for the material classification test.

Artificial Neural Network

The distance classification neural network has been implemented using the *Tensorflow* framework. The recorded data was trained using a feed-forward network with 3 hidden layers. Each hidden layer consists of a set of fully connected neurons. All hidden neurons used the rectified linear unit (ReLu) activation function [17], the network was trained using backpropagation [18] method and the Adam optimizer [19].

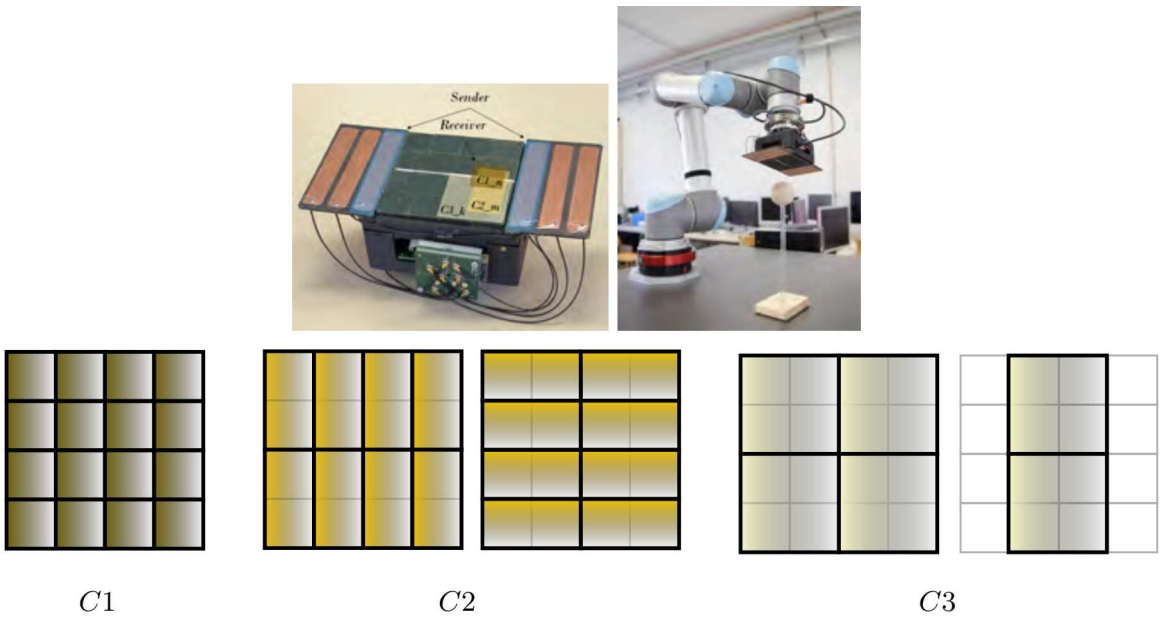

Fig. 5. Second sensor setup for classification of materials using machine learning. Top Left: The end-effector featuring three sensor modules: two 4×2 modules in the middle configured in receive mode and one module driving up to six electrodes in send mode. The PCB with the analog and digital electronics for the third module is visible in the front. The three modules are connected to the same I2C bus; Top Right: Setup with an Universal Robot with the sensors mounted on an end-effector. Similar to set-up shown in Fig. 3, the robot is used to perceive objects in its workspace. In this set-up it is used to classify them according to their permittivity or conductivity; Bottom: Illustration how the flexible spatial resolution is used to select single electrodes $C1_n$ with $n \in \{1, \ldots, 16\}$, configurations of two electrodes combined $C2_m$ with $m \in \{1, \ldots, 16\}$ and configurations of four electrodes combined $C3_k$ with $k \in \{1, \ldots, 6\}$.

The data, that was collected during the movement (s. Fig. 6) was shuffled and split into training and testing sets, the cross validation technique [20, 21] was performed with 5 folds (k=5), meaning one of the k subsets is used as the test set and the other k-1 subsets were combined to form a training set. The training algorithm had to run from scratch k different times. In the end, the average root mean squared errors was computed across all k folds.

Results

Multiple configuration were tested and per configuration 18246 data samples were generated. In [5] this is discussed more in detail. To give an idea two configuration are exemplary discussed and presented here. In a first notion the sensor signal of 3 different electrodes were used as feature input. This is based on the idea that triangulation requires at least 3 measurements to identify a location. The score that could be reached by this idea was 51.49%. Figure 7 on the left clearly shows, that distances close to the sensor can be distinguished quite good, but far distances led to misclassifications.

In summary we ended up using all available sensor measurements, i.e. all single sensor electrodes and all the combined ones ($E00 - E15$ and $qE00 - qE05$, s. Fig. 4) as input features. We got therefore a feed-forward backpropagation network with 22 inputs, 14 outputs for corresponding distances and 3 hidden layers with 80-40-20 neurons respectively. It yields after using cross-validation and tuning manually the hyper-parameters the highest classification score of all configurations with a value of 94.87%.

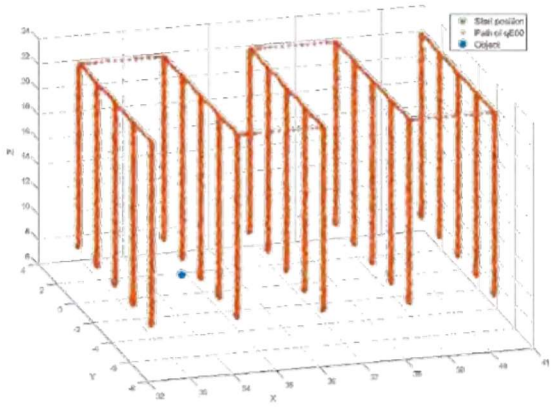

Fig. 6. Recording of the training data: The end-effector is moved over the object. At equidistant positions the end-effector moves downwards in direction of the object (s. Fig. 3). Based on the ability of the sensor to change the spatial resolution by combining electrodes, the sensor-data of single electrodes and of combined electrodes (s. Fig. 4) are recorded while moving.

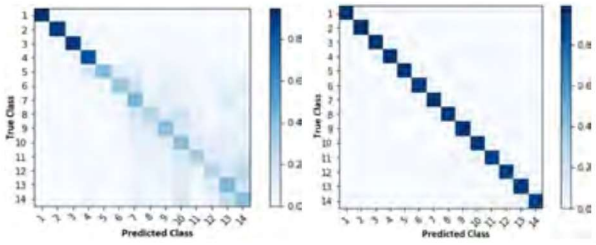

Fig. 7. Left: Using sensor information of three electrodes / electrode combinations as input allows a good classification for small distances but fails for far distances; Right: using all electrodes and all combinations (total of 22 sensor streams) lead to good classification results even for far distances.

Being this the first time for us to apply an ANN to our sensor data, the results were quite promising. Especially as the range for distance measurement was nearly doubled. Overall - for the given setup - the distances could be much more precisely measured and identified using ANNs than by using the original model-based approach.

4.2 Experimental Setup: Material classification

Encouraged by the previous results using ANNs for distance classification, a second way of exploiting ANNs and their classification abilities was investigated. Basic idea of this experiment was to classify materials based on their relative permittivity. The relative permittivity $\varepsilon_r(\omega)$ is depending on the frequency of an exciting electrical field they are in. As our sensors create such an electric field and are capable to use different exciter frequencies it was obvious step to try to exploit this capability.

Objects consisting of different materials (s. Table 1) were used to test the concept.[3]. All experiments were done in the laboratory by constant ambient temperature and humidity.

The distance between the electrode array and the top of the objects was kept to 2 mm during the measurements. Similar to the distance calculation in the previous Section

[3] The table is an excerpt of the values found in
http://www.kayelaby.npl.co.uk/general_physics/2_6/2_6_5.html

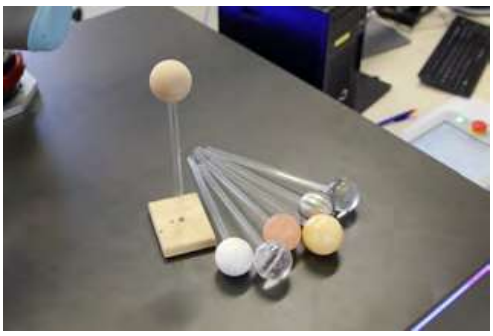

Fig. 8. Balls with diameter of $5cm$; Test objects of different Materials, one ball each

Material	Relative Permittivity ε_r
Styrofoam[22]	1.03
Glass (quartz)	3.8
Salt (NaCl)	6.1/5.9
Marble	8.0
Wood (Beech 16% water)	9.4/8.5
Tap water	80.1

Table 1. relative permittivity of the used test materials

the end-effector was moved in a meander path over the objects enclosing the borders of the receiver array (s. Fig. 9). This path was iterated ten times while the data was collected. In the training phase 74033 samples of all material were split in proportion 8/2 for training/validation. Additional 18512 samples were recorded for test. Every sample is a frame that contains the sensor values for the various electrode combinations and frequencies. Its size could variate depending on the selected combinations.

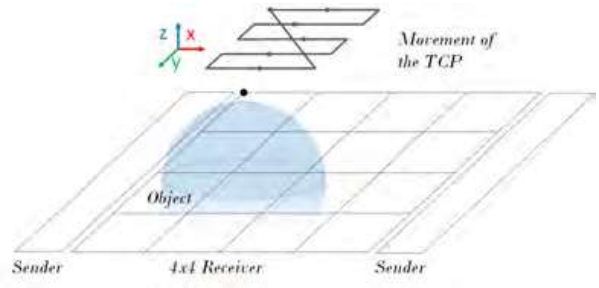

Fig. 9. Initial position of the end-effector and its path

Artificial Neural Network

The material recognition neural network was also implemented in *Tensorflow*. The recorded data was trained using a feed-forward neural network (ANN). For the ANN, the number of the input neurons was defined as the size of the data frames, hence by the selected electrode combinations and frequencies for each data set. The input was then forwarded through a series of *ReLU-layers*, where a dropout rate of 10% had been set. Lastly, the data was fed to a *softmax* output layer, whose size equaled the amount of materials trained for. In addition to introducing dropout to all hidden layers, the weights were also modified through L2 regularization to further decrease overfitting. Updates to weights

were done in mini-batches of 300 and optimized by the Adam optimizer [19]. To further prevent overfitting, every five epochs, the validation set's accuracy was calculated and training was prematurely ended when this accuracy exceeded a threshold of 0.98. Furthermore, a patience period of ten epochs to stop training was set, which counted up if the validation loss did not decrease compared to the last best loss. The best results were achieved by setting the hidden layer size to two layers with 400 units each. The initial learning rate was set to 0.001. The Hyperparameters are listed in Table 2. Those were determined in a previous experimental run and showed best results for all data sets. The hyper-parameter do not variate between the data sets.

Hidden layers	400, 400
Batch size	300
Learning rate	0,001
L2 beta	0,1
Dropout	0,1

Table 2. Hyperparameters of the ANN

Results

The measurement was performed for all seven objects[4]. For each object about 13100 data frames were collected. Due to the air-like relative permittivity of "styrofoam" this object acted as air.

Set	3
Variation	$C2_m$
	89 kHz,178 kHz
Input	32
Epochs trained	25
Test accuracy	94.2%

$$\begin{bmatrix} me & sa & ma & wo & gl & wa & sf \\ 2665 & 20 & 0 & 0 & 8 & 2 & 0 \\ 2 & 1835 & 822 & 0 & 1 & 0 & 0 \\ 0 & 223 & 2436 & 0 & 0 & 0 & 0 \\ 0 & 0 & 0 & 2632 & 0 & 0 & 0 \\ 0 & 0 & 0 & 0 & 2640 & 0 & 0 \\ 0 & 0 & 0 & 0 & 0 & 2607 & 0 \\ 0 & 0 & 0 & 0 & 3 & 0 & 2627 \end{bmatrix}$$

Accuracy	94.2%
Precision	[99.3 69.0 91.6 100 100 100 100]
Recall	[99.9 88.3 74.8 100 100 100 100]

The network was fed with different combinations of the measurement regarding the electrode combinations and the exciter frequencies. In [6] the different combinations are discussed in detail. It turned out that the $C2_k$ combination showed the best results. We believe that the $C1_n$ and $C3_k$ do not provide enough information. While $C1_n$ has the highest spatial resolution, its electrodes are relatively small and less sensitive, with a lower Signal-to-Noise ratio (SNR). On the other hand, $C3_k$ has the highest sensitivity,

[4] me: metal, sa: salt, ma: marble, wo: wood, gl: glass, wa: water, sf: Styrofoam

but also the lowest spatial resolution. The $C2_m$ configuration is placed in between $C1_n$ and $C3_k$ and therefore seems to combine for the given setup the needed spatial resolution and increased sensitivity in an optimal way.

5 Conclusion

In this work we have summarized and compared our previous work about two examples of beneficially using ANNs in combination with our tactile proximity sensors. Specially we did focus on the proximity sensing ability of these sensors.

In the first approach [5] we could show, that distance classification can be done using an ANN in a very straightforward way. For the given setup this approach yields better results regarding the measurable distances. With the original model-based approach we could detect and identify distances up to somehow 8cm. The ANN approach described here, nearly doubled the range and allowed us to extended the feasible measuring range up to 14cm.

The second approach [6] is targeting material recognition. It makes use of the abilities of our sensors to measure with multiple frequencies and to flexible combine electrodes allowing to configure the spacial resolution of the sensors. Correspondingly to the distance approach an artificial neural network for the classification was used. The essence of the work was to perform the measurement with various combination of the sensor features which can provide sufficient information to recognize material without further information. For the evaluation, data has been collected by measuring seven object of different materials with variation of electrode combinations and two driving frequencies. The best recognition result with an accuracy of 94% was reached through the $C2_m$ electrode combination and both frequencies. The experiment shows that the combination of various electrode shapes and driving frequencies is promising for material recognition.

Since all experiments were done in the laboratory by constant ambient temperature and humidity. Further investigation in operating conditions should also be done.

References

1. Jiang, L.T., Smith, J.R.: Seashell effect pretouch sensing for robotic grasping. In: 2012 IEEE International Conference on Robotics and Automation. (May 2012) 2851–2858
2. Koyama, K., Suzuki, Y., Ming, A., Shimojo, M.: Integrated control of a multi-fingered hand and arm using proximity sensors on the fingertips. In: 2016 IEEE International Conference on Robotics and Automation (ICRA). (2016) 4282–4288
3. Schlegl, T., Kröger, T., Gaschler, A., Khatib, O., Zangl, H.: Virtual whiskers #x2014; Highly responsive robot collision avoidance. In: 2013 IEEE/RSJ International Conference on Intelligent Robots and Systems. (November 2013) 5373–5379
4. Alagi, H., Navarro, S.E., Mende, M., Hein, B.: A versatile and modular capacitive tactile proximity sensor. In: 2016 IEEE Haptics Symposium (HAPTICS). (April 2016) 290–296
5. Madani, B., Alagi, H., Hein, B., Aurélie Arntzen, A.: Machine Learning Algorithms for Capacitive Tactile Proximity Sensor Data, Birmingham, USA (November 2017)
6. Alagi, H., Heilig, A., Navarro, S.E., Kroeger, T., Hein, B.: Material recognition using a capacitive proximity sensor with flexible spatial resolution. In: 2018 IEEE/RSJ International Conference on Intelligent Robots and Systems (IROS), IEEE (2018) 6284–6290
7. Mayton, B., LeGrand, L., Smith, J.R.: An Electric Field Pretouch system for grasping and co-manipulation. In: 2010 IEEE International Conference on Robotics and Automation. (2010) 831–838
8. Wistort, R., Smith, J.R.: Electric field servoing for robotic manipulation. In: 2008 IEEE/RSJ International Conference on Intelligent Robots and Systems. (Sep. 2008) 494–499

9. Navarro, S.E., Schonert, M., Hein, B., Wörn, H.: 6d proximity servoing for preshaping and haptic exploration using capacitive tactile proximity sensors. In: 2014 IEEE/RSJ International Conference on Intelligent Robots and Systems. (September 2014) 7–14
10. Yamada, Y., Tsuchida, N., Ueda, M.: A proximity-tactile sensor to detect obstacles for a cylindrical arm. Journal of the Robotics Society of Japan **6** (01 1988) 292–300
11. Lumelsky, V.J., Cheung, E.: Real-time collision avoidance in teleoperated whole-sensitive robot arm manipulators. IEEE Transactions on Systems, Man, and Cybernetics **23**(1) (January 1993) 194–203
12. Kirchner, N., Hordern, D., Liu, D., Dissanayake, G.: Capacitive sensor for object ranging and material type identification. Sensors and Actuators A: Physical **148**(1) (November 2008) 96–104
13. Yunus, M.A.M., Mukhopadhyay, S.C., Ibrahim, S.: Planar Electromagnetic Sensor Based Estimation of Nitrate Contamination in Water Sources Using Independent Component Analysis. IEEE Sensors Journal **12**(6) (June 2012) 2024–2034
14. Wang, X., Wang, Y., Leung, H., Mukhopadhyay, S.C., Tian, M., Zhou, J.: Mechanism and Experiment of Planar Electrode Sensors in Water Pollutant Measurement. IEEE Transactions on Instrumentation and Measurement **64**(2) (February 2015) 516–523
15. Kimoto, A., Fujisaki, S., Shida, K.: A proposal of new contactless layered sensor for material identification. Sensors and Actuators A: Physical **155**(1) (October 2009) 33–38
16. Mühlbacher-Karrer, S., Gaschler, A., Zangl, H.: Responsive fingers #x2014; capacitive sensing during object manipulation. In: 2015 IEEE/RSJ International Conference on Intelligent Robots and Systems (IROS). (September 2015) 4394–4401
17. LeCun, Y., Bengio, Y., Hinton, G.: Deep learning. Nature **521**(7553) (May 2015) 436–444
18. Dai, Q., Liu, N.: Alleviating the problem of local minima in backpropagation through competitive learning. Neurocomputing **94** (2012) 152–158
19. Kingma, D.P., Ba, J.: Adam: A method for stochastic optimization. CoRR **abs/1412.6980** (2014)
20. Kohavi, R.: A study of cross-validation and bootstrap for accuracy estimation and model selection. In: Proceedings of the 14th International Joint Conference on Artificial Intelligence - Volume 2. IJCAI'95, San Francisco, CA, USA, Morgan Kaufmann Publishers Inc. (1995) 1137–1143
21. Shao, J.: Linear model selection by cross-validation. Journal of the American Statistical Association **88**(422) (1993) 486–494
22. Visser, H.J.: Appendix D: Physical Constants and Material Parameters. In: Antenna Theory and Applications. John Wiley & Sons, Ltd (2012) 243–244